BULLETIN OF THE POLISH ACADEMY OF SCIENCES
TECHNICAL SCIENCES, Vol. 69, No. 1, 2021, Article number: e136037
DOI: 10.24425/bpasts.2021.136037

The effect of protrusions on the initiation of partial discharges in XLPE high voltage cables

Mohammad ALSHAIKH SALEH[1,2*], Shady S. REFAAT[2], Marek OLESZ[3], Haitham ABU-RUB[2], and Jarosław GUZIŃSKI[3]

[1] Department of Electrical and Computer Engineering, Technical University of Munich, 80333 Munich, Germany
[2] Department of Electrical and Computer Engineering, Texas A&M University at Qatar
[3] Departement of Electrical Engineering, Gdansk University of Technology, ul. Gabriela Narutowicza 11/12, 80-233 Gdańsk, Poland

Abstract. This paper is focusing on 3D Finite Elements Analysis (FEA) based modelling of protrusions as defects or imperfections in the XLPE high voltage cable. This study is aiming to examine the impact protrusions have on the initiation of partial discharges. Spherical and ellipsoidal protrusions with different sizes at the conductor screen of the high voltage cable is an essential content of this paper. In addition, a spherical gas-filled void is placed inside and outside the protrusions, and a water tree produced from protrusions is under consideration. The partial discharge influence taking place at the protrusions and the stress enhancement factor is determined for all the variations mentioned to quantify the rise in the inception of partial discharges due to the protrusions.

Key words: FEA; protrusions; XLPE; water trees; partial discharge; void; space charge; stress enhancement factor.

1. Introduction

XLPE insulation is regularly employed for HV cables because it possesses exceptional electrical and mechanical features [1, 2]. Yet, aging of XLPE insulation occurs as a result of variations in the properties it possesses when subjected to a change in permittivity and a distorted electric field [2, 3]. This can be substantiated by the consequence of the initiation of partial discharges that would eventually cause the deterioration of the insulation until a total failure of the cable [4–7]. Aging of the XLPE insulation impacts electrical strength, the dielectric loss factor, and the resistivity of the insulation. Subsequently, continuous monitoring and safety procedures of the XLPE are vital to evade any malfunction occurring in the power cable [6]. One of the critical reasons for the degradation of power cables are the defects/irregularities in the insulation [1–8]. The irregularities are usually gas-filled voids and protrusions as shown in Fig. 1.

These irregularities are bases of partial discharges in XLPE that plays a role in the deterioration of HV equipment resulting in a breakdown [2, 5–7]. Three irregularities are taken into account in this paper. Those irregularities entail protrusions (main defect under investigation), vented water trees, and cavities (or voids).

These irregularities distort the electrical field across the insulation increasing the degree of non-uniformity of the field. Moreover, the conduction and polarization properties are impacted, and the intensity of partial discharges occurring rises, which places the HV cable in a susceptible condition [2, 8–9].

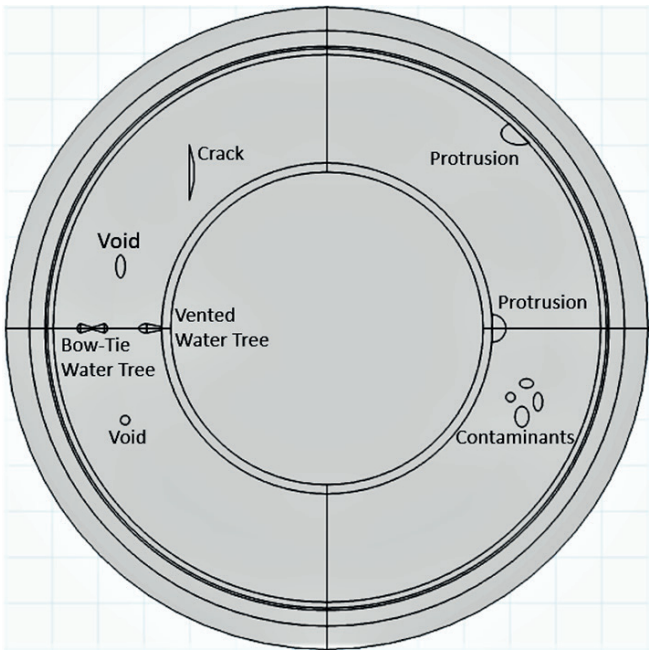

Fig. 1. Defects found in high voltage cables with XLPE insulation

The space charges tend to accumulate at the defects which are also attributed as an influencing factor for high electrical stresses within the XLPE insulation [10–12].

This paper involves the grouping of more than one defect in the same locality of XLPE and studying their effect. This is crucial because most papers study the impact on the electric field distribution merely due to one kind of defect and they don't exemplify the consequence of having different combinations of defects in the same vicinity in XLPE. Furthermore, to

*e-mail: mohammedalshaikhsaleh@hotmail.com

Manuscript submitted 2020-05-28, revised 2020-09-05, initially accepted for publication 2020-09-10, published in February 2021

fully comprehend the effect of more than one imperfection on the inception of partial discharges, their structures are altered.

Having voids inside and outside the protrusions, and vented water trees grown from protrusions is also not profoundly researched as most papers just investigate the protrusions on its own which is not always the case in practical situations. The reference [8] is on the effect of protrusions in HVDC cables and considers the effect of spherical and spheroidal protrusions on the electric field and from that determine the changes in the stress enhancement factor. Therefore, this paper attempts to build on that by considering voids inside and outside the protrusions and vented water trees grown from protrusions mentioned previously at the conductor screen which is a configuration rarely investigated although it happens in practice. Consequently, these alterations mentioned will be taken into account for practical applications to take the appropriate mitigations versus the weakening of power cables due to these defects.

The **main contribution** is that the edge of the protrusion at the conductor screen and the different permittivity between the conductor screen and the XLPE insulation causes the electric stress in the insulation to rise. That leads to the initiation of partial discharges at the edge and if the space charges accumulated at that edge possess a certain amount of energy then that will cause treeing to occur. Therefore, the proposed paper considers vented water trees growing from protrusions as the process described proves that water trees can grow in the presence of protrusions. Otherwise, if the appropriate countermeasures are not considered, the discharge channel will grow to the opposite electrode until the two electrodes are electrically connected and that ultimately will lead to the breakdown of the insulation material and a huge failure of the power cable. In addition, it is only possible for the inception of water trees to take place if moisture is present in the insulation. This can occur in regions with humidity. Therefore, the paper attempts to consider the effect that water trees have on the cable insulation as part of the paper contribution.

This paper also attempts to consider gas-filled voids as many researchers still consider air-filled voids rather than gas-filled voids. Due to the development of cables and the triple extrusion that takes place, it is not possible to introduce air, however, gas inclusions can take place from by-products of the cross-linking process. The production of cables with XLPE insulation has been improving in the last decades as to ensure that failure of the insulating medium is brought to a minimum. The production of cables nowadays follows a process of extruding three main layers in cables: the conductor screen, insulation screen, and the XLPE insulation. This process manufactures extruded insulated cables which makes it almost impossible to have air, dust, or other irregularities present in the insulating medium. However, some of the aforementioned defects might take place due to destructive factors or errors done in the manufacturing process.

This paper focuses on an FEA modelling of protrusions as defects or imperfections in an XLPE high voltage cable to examine the impact they have on the electric field distribution. Spherical and ellipsoidal protrusions will be investigated with different sizes at the conductor screen of the power cable. A spherical gas-filled void will be placed inside and outside the protrusions, and a vented water tree grown from the protrusions will be considered. The impact on the inception of partial discharges in the presence of protrusions and the stress enhancement factor will be determined for all the variations mentioned as it will quantify the rise in the initiation of partial discharges due to the protrusions. It should be noted that, in the present design of HV cables consists of the conductor screen, the XLPE insulation, and the insulation screen. Those are extruded all together in one process to create a powerful bond between the screens and the XLPE. Ultimately, this will avoid the presence of a cavity between these screens. However, a cavity can still be found in the event that destructive factors take place during the installation of the HV cable.

The paper is arranged as follows: Section 2 explains the origin and development of PDs. Section 3 exemplifies the AC and DC void insulation models. Then Section 4 explains the types of defects studied in this paper. Next, Section 5 explains the PD COMSOL 3D modeling and gives an outline of the simulations done regarding the variations done with the defects. In Section 6, the FEA data and analytical solutions are shown and exemplified.

2. Partial discharge origin and development

PDs are usually affected by factors such as humidity and temperature (Paschen's law), mechanical influence, and imperfections in the insulating medium. The imperfections or defects usually entail electrical and water treeing, gas-filled voids, and electrodes with floating potential.

The development of PDs is also a result of the permittivity changes between a defect and the dielectric medium in the cable. Consequently, this leads to the chemical degradation of the insulation material and field ionization due to the collision of molecules arise, resulting in the avalanche effect [13]. Therefore, if monitoring techniques were not used, a breakdown of the cable dielectric material would take place. PD in high voltage cables can be subcategorized into surface, internal, and corona discharges. For instance, if a gas-filled void is considered as the defect under investigation the inception PD would be as a result of gas composition, electronegative gases, and surface erosion. These processes would ultimately lead to changes in pressure, conductivity, temperature, surface roughness, etc. [13]. Consequently, having a void will aid the inception of electrical trees and will make the consequences more dire if it is in the vicinity of a protrusion as the space magnitude increases towards protrusions and voids leading to a higher electric stress, which in turn decreases the breakdown voltage [14].

3. AC and DC void discharge models

When detecting partial discharges with the application of AC and DC voltages, differences in the mechanisms take place. At AC, PD activity can be represented by capacitors to characterize the properties of the XLPE insulating medium [4]. The commonly utilized model for solid dielectrics with the presence of

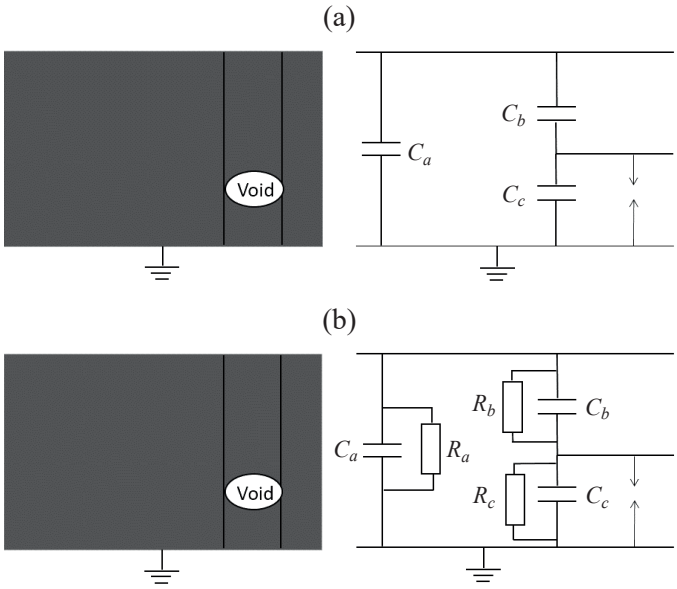

Fig. 2. Equivalent void discharge model with (a) AC voltage source (b) DC voltage source

voids is the three-capacitor model (or the abc-model) as shown in Fig. 2a. It gives a convenient depiction of internal partial discharges. The capacitor C_c represents the void, C_b the insulation in series with the void, and C_a represents the rest of the insulation. When the electric field surpasses the PD inception level in the cavity, then a PD is the outcome [15]. Therefore, C_c (of the void) will discharge, and a voltage drop across the void occurs.

When a DC voltage (constant) is applied, the abc model would arrive at a steady-state condition and the activity will end as opposed to the AC condition. As shown in Fig. 2b, the PD model for the DC voltage source is amended to take into account the charge dissipation due to the void into the dielectric [15]. The amendment was accomplished by adding a resistor (R_a, R_b, and R_c) in parallel to each capacitor. The rate for which PD occurs depends on the voltage level applied and the conductivity of the insulating medium at the vicinity of the void.

A distinction between HVDC and HVAC cables needs to be addressed. Having the same distribution of electric field in the XLPE insulation, for AC and DC systems, cannot be the case. In the isolation of the HVAC cables, the maximum electric strength is in isolation at the conductor screen. However, the field distribution in the HVDC cable is dependent on the resistivity or the conductivity of the XLPE insulating medium. The only time the electric field distribution is the same, for both HVDC and HVAC cables, is when the cable systems are energized at zero load and with no change in the temperature.

4. Types of defects investigated

Protrusions are usually located in conductor and insulation screens (semi-conductive screens) and are found to be a huge contributor to the occurrence of high electrical stresses in the XLPE insulating medium and the semi-conductive screens. They could occur because of limitations in the manufacturing of these cables or mistakes done while installing them. The size and shape of the protrusions should also be considered because the sharper the protrusion is for instance then a higher electrical stress would be the outcome due to a higher space charge density accumulated at the sharp area of the protrusion giving a higher stress enhancement factor which is defined as the ratio of the maximum electric field due to the protrusion and the average electric field in XLPE disregarding the protrusion [8].

Gas-filled cavities (or voids) is one of the most common partial discharge defects found in power cable insulation [16–18]. They usually have a permittivity of $\varepsilon_r = 1$ depending on the location of the cable and the environment surrounding it. Since the cavity has a relative permittivity of 1 then high electrical stress would be the outcome because this cavity has a lower permittivity XLPE ($\varepsilon_r = 2.3$) [14].

Water treeing is a phenomenon that degrades the insulation material in such a way that it forms structures in XLPE when an electric/internal stress is applied. This ultimately leads to electrical treeing and a breakdown of the insulation material to take place in HV cables. Water trees have the propensity to propagate as diffuse structure that as appears to be similar to a tree [15].

Vented water trees are originated from the semi-conductive shields and because of their propensity to keep growing, they cause a breakdown to occur in water treed samples [19–23]. Vented water trees can also cause the release of an internal gas pressure at the semi-conductive layers. Breakdown is to then take place as the water trees are transformed into electrical trees at the region where the tip of the water tree is situated. This is because of the high charge accumulation which gives a rise in the PD activity. When a transformation happens, the electrical tree will distribute along the insulation and a channel will be formed with the electrodes and initiate the damage of the XLPE material [8].

5. Power cable modelling using FEA

A 220 kV HVDC cable with an XLPE insulation is simulated by the FEA. It has a thickness of 23.6 mm with the irregularities mentioned. Three instances are simulated to comprehend the variation of the partial discharge initiation. To calculate the increase in the stress in the presence of protrusions the stress enhancement factor should be determined [8] as shown in Eq. (1) below:

$$\prod = \frac{E_{max}}{E_0} \tag{1}$$

whereby E_{max} is the maximum electric field strength due to the presence of the protrusion and E_0 is the average electric field strength in XLPE from the tip of the protrusion without considering the protrusion. Three cases are investigated to comprehend the PD inception to a greater extent and the changes

in the stress enhancement factor. The electric field in a cable without defects is described by (2):

$$\vec{E}(r) = \frac{V_0}{rln\left(\frac{r_e}{r_i}\right)} \cdot \hat{r} \tag{2}$$

where V_0 is the applied voltage in the conductor, r is the distance to the center conductor, r_i is the radius of the inner insulation, r_e is the radius of the outer insulation, and $\hat{r}$ is a unit vector directed towards the conductor.

The electric field with the presence of a protrusion can be expressed as for the case of Fig. 3 (See (3)).

$$\vec{E}(r) = \frac{V_0}{rln\left(\frac{r_e}{r_i}\right)}\left(1 + \frac{2a^3}{(r-r_i)^3}\right) \cdot \hat{r} \tag{3}$$

The electric field with the presence of an ellipsoidal protrusion can be obtained from Table 2 [24].

The first case entails a spherical and an ellipsoidal protrusion (semi-conductive) investigated with different sizes at the conductor screen of the power cable. With regards to the spherical protrusion, it will be located at the conductor screen then following sizes will be examined: 1 mm to 6 mm. The m is known as the sharp factor and it is defined as the ratio of the protrusion's height a and its radius c (m = a/c*)* as shown in Fig. 3. Values of m investigated are m = 2 to m = 6 where c = 0.5 (constant for all the m values). For these two protrusions, the stress enhancement factor and the electric field distribution will be obtained to observe the severity of the partial discharges as parameters of the protrusions are changed. The dimensions and the materials of the cable used can be seen in Fig. 4 and Table 1.

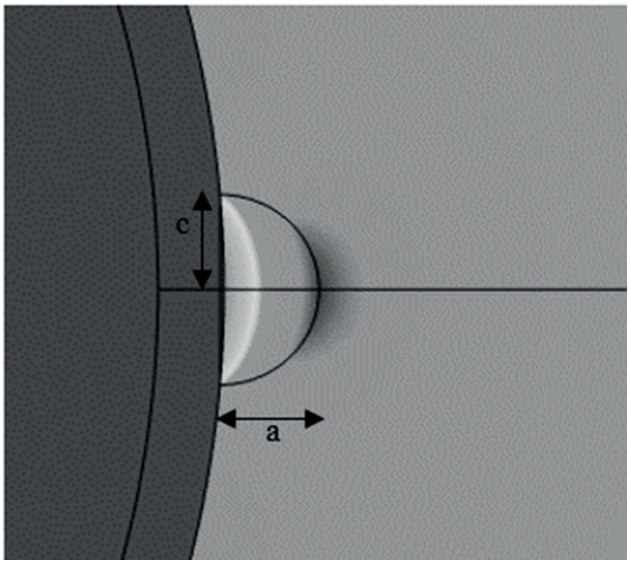

Fig. 3. The geometry of a typical protrusion

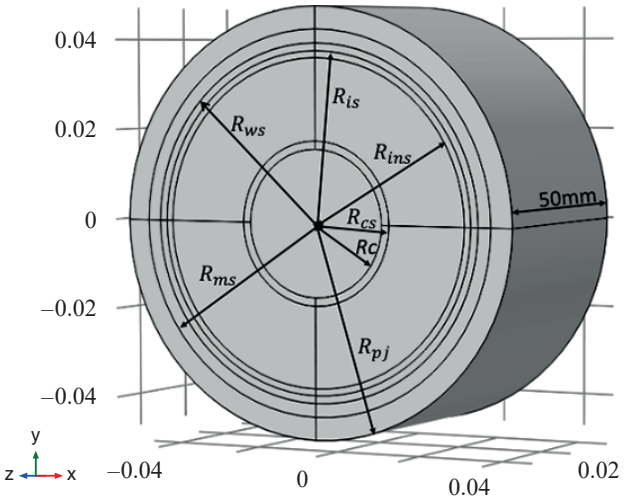

Fig. 4. XLPE power cable under investigation

Table 1
Details of the cable used

Description	Radius [mm]	Material
Conductor	$R_c = 32.15$	Copper
Conductor Screen	$R_{cs} = 34.35$	Graphite screen
Insulation	$R_{ins} = 58.4$	XLPE
Insulation Screen	$R_{is} = 59.85$	Graphite screen
Wired Screen	$R_{ws} = 60.4$	Kapton H
Metallic Sheath	$R_{ms} = 64.15$	Lead
PVC Jacket	$R_{pj} = 70$	PVC

The second case is a spherical gas-filled void with a radius of 50 μm will be placed inside and outside the 3 mm spherical protrusion at the conductor screen.

The third case is a 1.5 mm long vented water tree grown from a 3 mm spherical protrusion at the conductor screen. Referring to the investigation made by Nakamura [25], the ε_r of the vented water tree varies exponentially from 5 (at conductor screen) to 2.3 at head (high charge density) of the defect.

6. Results and discussions

It can be seen from Fig. 5 that the electric field has a higher value in the boundary of the conductor and declines exponentially with distance. The maximum electric field strength is 6.7 kV/mm at the boundary of the conductor. Ultimately, this paper attempts to see the distortion of the electric field and how that affects the stress enhancement factor due to the defects under investigation mentioned in Section 4.

6.1. Analysis of the spherical and ellipsoidal protrusions (Case 1). It is assumed that the space charge density is kept constant at 0.124 C/m^3 for the defects investigated [2]. With

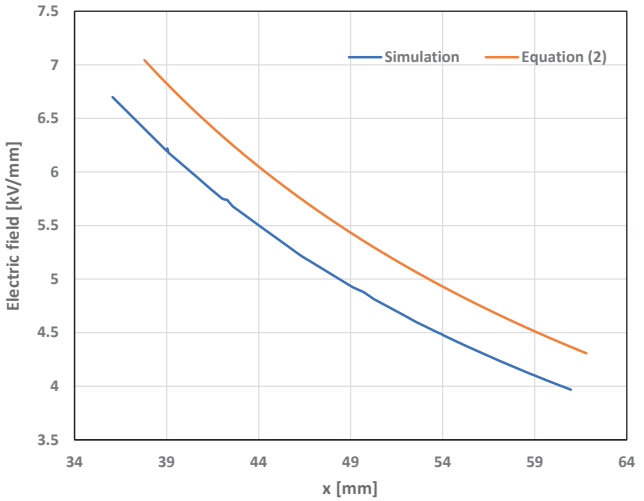

Fig. 5. Electric field plot of the healthy 220 kV power cable utilized with respect to the distance from the inner semi-conductor

regards to the 1 mm spherical protrusion located at the conductor screen, a high electric field is observed at the tip because of the high space charge density that usually accumulates at sharper regions as shown in Fig. 6. The space charges accumulated could be due to numerous reasons such as irreversible polarization, diffusion and attachment of charge carriers within the insulation [2]. In Fig. 7 a plot of the electric field as

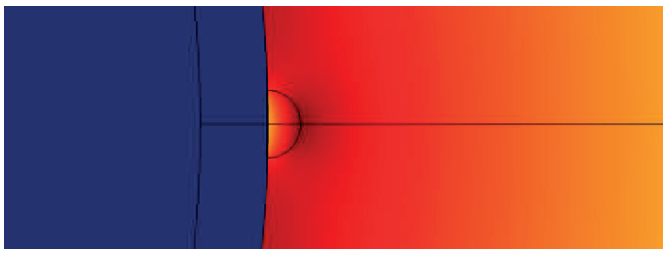

Fig. 6. Electric field distribution of the 1 mm spherical protrusion located at the conductor screen

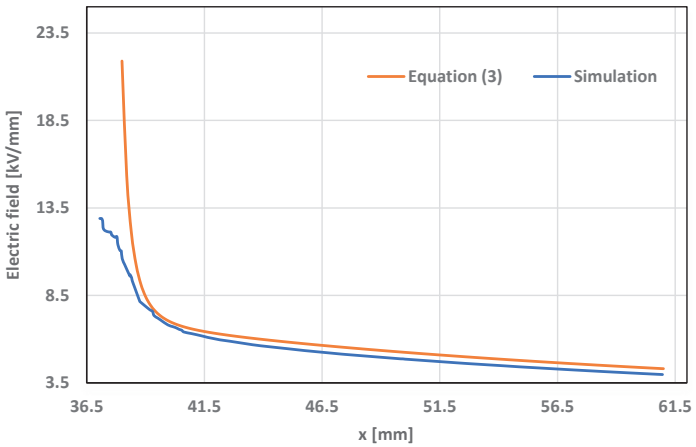

Fig. 7. Electric field plot of the 1 mm spherical protrusion located at the conductor screen

a function of the cable's diameter is acquired in the presence of the 1 mm spherical protrusion at the conductor screen. In addition, (2) was plotted to show the validity of the simulation results obtained.

Firstly, the electric field is 0 kV/mm for positions 36 mm and less, because that is where the conductor is located. However, at the tip of the protrusion, it can be seen that the electric field is at its peak (at 37 mm) with a value of 12.9 kV/mm. Comparing this with Fig. 5 (when the cable was free of defects) the peak was at 6.7 kV/mm, so an increase of the electric field was the outcome because of the increase in the space charge density in the vicinity of the protrusion. The increase in the space charge density would then lead to more ionization and consequently becomes more susceptible to the occurrence of the avalanche effect until a breakdown takes place of the conductor screen and the XLPE insulation. The edge of the protrusion at the conductor screen and the different permittivity between the conductor screen and the XLPE insulation causes the electric stress in the insulation to rise. Then that leads to the initiation of partial discharges at the edge and will also cause treeing to occur. This is why this paper considers vented water trees growing from protrusions as the process described proves that water trees can grow in the presence of protrusions. Otherwise, if the appropriate countermeasures are not taken the discharge channel will grow to the opposite electrode until the two electrodes are electrically connected and that ultimately will lead to the breakdown of the insulation material and a huge failure of the power cable. Moreover, the electric field distorts because the electrical conductivity is dependent on the temperature as well. Since the temperature and the electric field is higher closer to the conductor then the electrical conductivity will increase causing the generation of more charges in the insulation material which ultimately distorts the electrical field to a higher degree of non-uniformity. Moving on, after 39.8 mm (from protrusion's tip) an exponential decay is observed of the electric field moving further away from the conductor and the protrusion. The same effect was also observed when the protrusion was 3 mm but an increase in the electric field (14.5 kV/mm) was the result as shown in Fig. 8.

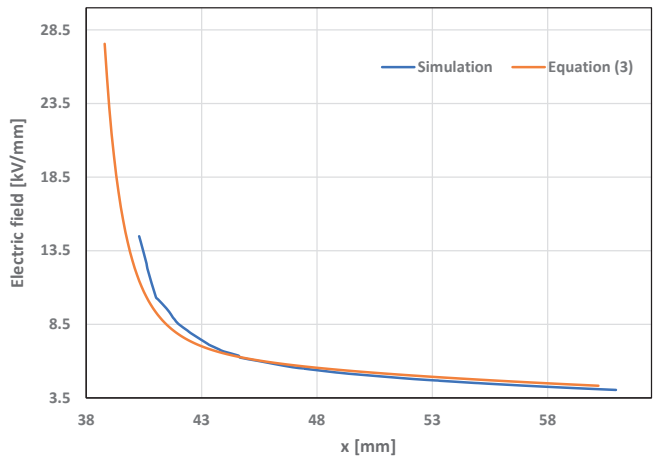

Fig. 8. Electric field plot of the 3 mm spherical protrusion located at the conductor screen

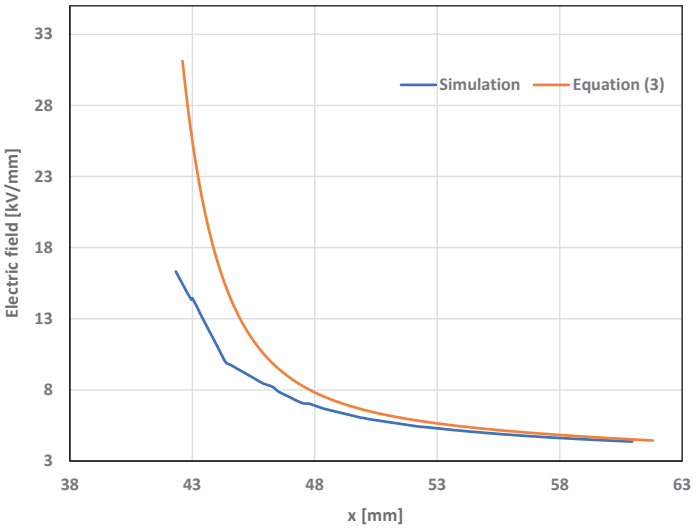

Fig. 9. Electric field plot of the 6 mm spherical protrusion located at the conductor screen

As shown in Fig. 9, the electric field was plotted for the 6 mm protrusion. At approximately 42.6 mm there was a substantial rise in the electric stress relative to the smaller protrusions. This is because of the edge that is prominent between the conductor screen and the protrusion, which created a higher charge accumulation. Therefore, this will cause treeing and an increase in the frequency of the partial discharges occurring, which substantiates the fact that vented water trees do grow from protrusions and as a result increase the electrical stresses and decrease the breakdown voltage.

Figure 10 shows the maximum electric field strength and stress enhancement factor obtained for a radius ranging from 1 to 6 mm for the spherical protrusion located at the conductor screen. As the radius (or size) of the protrusion increases, the maximum electric field strength also increases with a linear behavior. This is because of a rise in the charge carriers generated in the insulation. Therefore, according to Fig. 10, the stress enhancement factor is proportional to charge carriers generated (higher electrical conductivity and heating) as the radius increases, so the high space charge density will distort the electric field even more with protrusions causing high temperatures (or heating) at the vicinity of the protrusions.

In Figs. 11–13 an increase in the electric field and the stress enhancement factor was the outcome because of the increase in the sharp factor m and size of the protrusion that generates more charge carriers at the tip. Thus, as a result, the stress enhancement factor or the electric field must rise. In other words, mobile electrons are absorbed by the anode (the ellipsoidal protrusion due to a sharper edge than a spherical protrusion) then positive space charge are left in the vicinity of the anode. After that the field in the space charge free region is increased which results

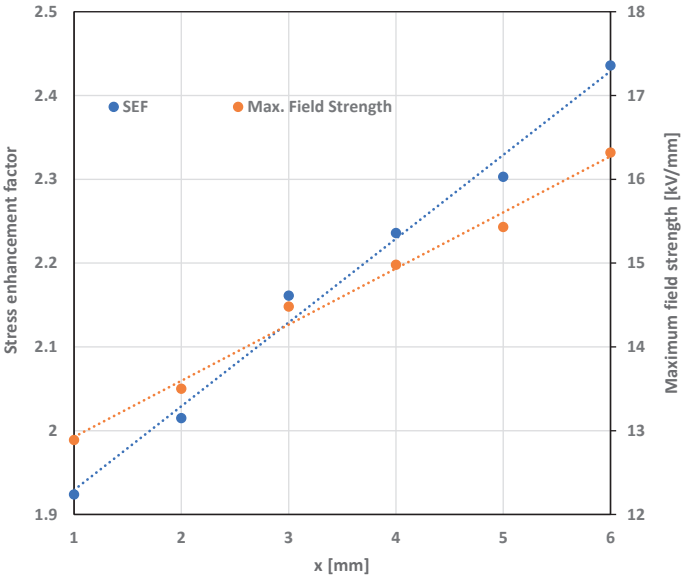

Fig. 10. Maximum electric field and stress enhancement factor plot as a function of the radius of the spherical protrusions located at the conductor screen

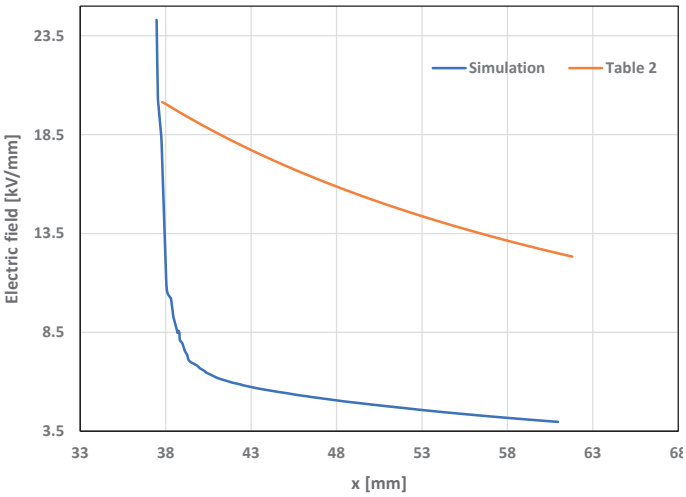

Fig. 11. Electric field plot of the ellipsoidal protrusion (m = 2) located at the conductor screen

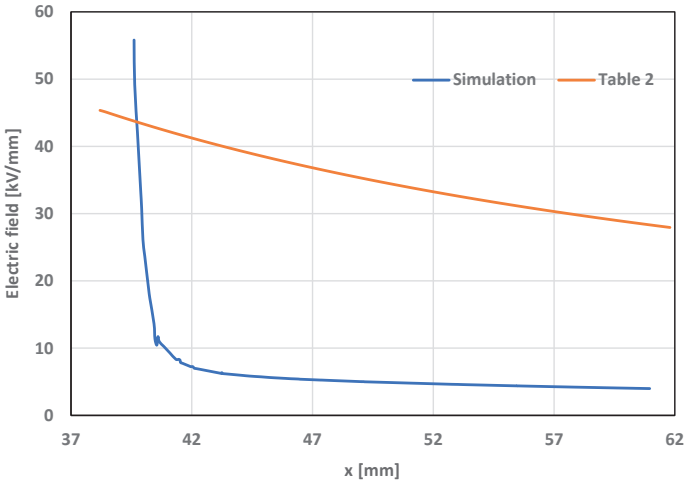

Fig. 12. Electric field plot of the ellipsoidal protrusion (m = 6) located at the conductor screen

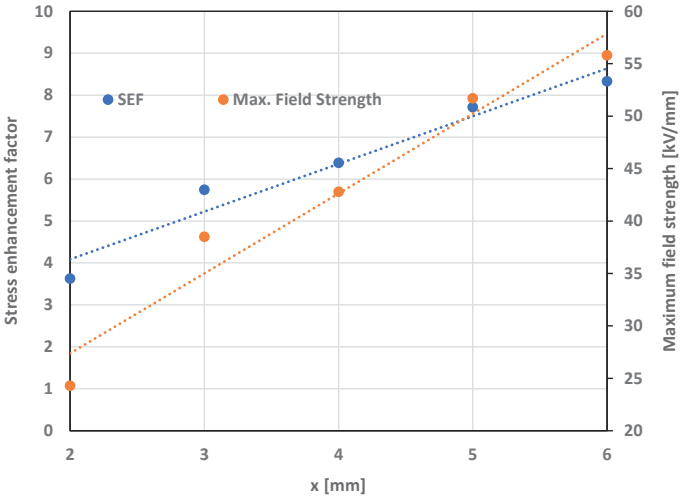

Fig. 13. Maximum electric field and stress enhancement factor plot as a function of the sharp factor of the ellipsoidal protrusions located at the conductor screen

in more ionization taking place. For a sharp factor of m = 2 the field strength was 24.3 kV/mm according to the simulation results and 20.1 kV/mm according to Table 1 which is close to the maximum field strength obtained from the simulation.

For the sharp factor of m = 6 the field strength increased rapidly due to the sharper edge which increased the concentration of the mobile electrons at that region. As a result, the electric field reached a peak value of 55.8 kV/mm according to the simulation and 45.4 kV/mm as shown in Fig. 12. In Fig. 13, the stress enhancement factor and the maximum field strength increased as the sharp factor reached higher values.

The equations plotted for the spherical protrusions gave similar results. With non-uniform cases it is more complicated to know exactly where and what is the distribution of charge, it can only be assumed. The simulation only shows the distribution of the electrical field at the moment of maximum voltage. Local charge density will fundamentally change the electrical field distribution as shown in the figures. Therefore, research is being done with regards to the influence of charge and polarity of voltage on the electrical field distribution and will be presented in the next paper.

Table 2
Stress enhancement factor [24]

	E [kV/mm]	Π
2a/c = 0 (without protrusion)	0.76	1
2a/c = 1	1.47	1.93
2a/c = 2	2.18	2.86
2a/c = 4	3.59	4.72
2a/c = 6	4.9	6.44

6.2. Analysis of protrusions with voids (Case 2). Figures 14 and 15 show that the 50 m void increases the electric field

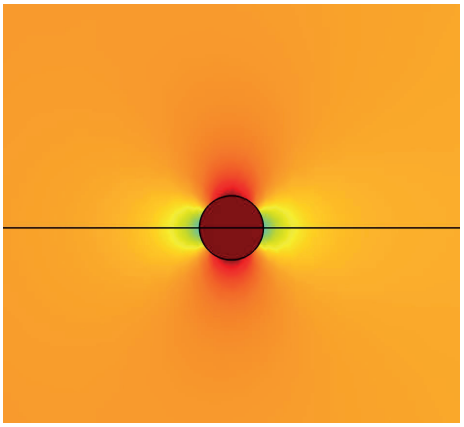

Fig. 14. Electric field distribution of the 50 μm gas-filled spherical void inside the 3 mm spherical protrusion located at the conductor screen

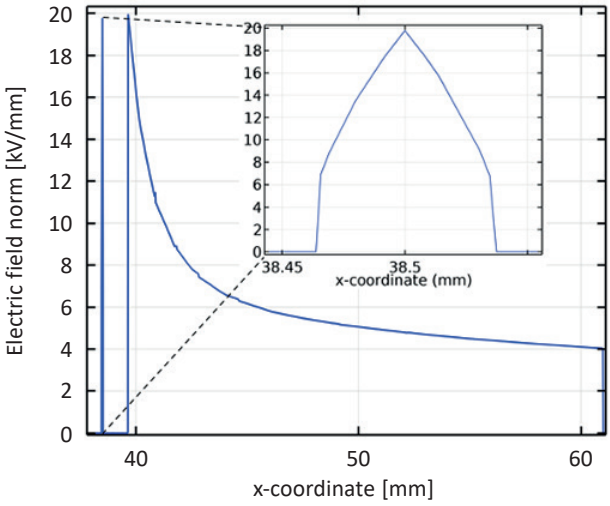

Fig. 15. Electric field plot of the 50 μm gas-filled spherical void inside the 3 mm spherical protrusion located at the conductor screen

drastically. This is due to a lower relative permittivity within the void causing this increase and because of that, the generation of space charges will also increase. However, when the cavity was outside as shown in Fig. 15; a larger electric field was observed due to the cavity and this is because there was a larger difference in the ratio of the permittivity of the void and the XLPE insulation (the void had a lower permittivity) as opposed when the void was inside the protrusion and this explains the large decrease of the electric field at the XLPE insulation material (at 41 mm) in Fig. 15. However, as shown in Fig. 16 at 40 mm the tip of the protrusion was there so a higher space charge density was in that region compared to the XLPE insulation. After that, when treeing is initiated due to space charges resulting from the field distortion of the protrusion, the XLPE insulation will be in a vulnerable situation. Partial discharges usually take place when the electric field strength is 3 kV/mm or more in the void which the case here is. As for the escalation in the stress enhancement factor, 4.93 was the result acquired when the cavity was outside the protrusion and 2.99 when inside which is

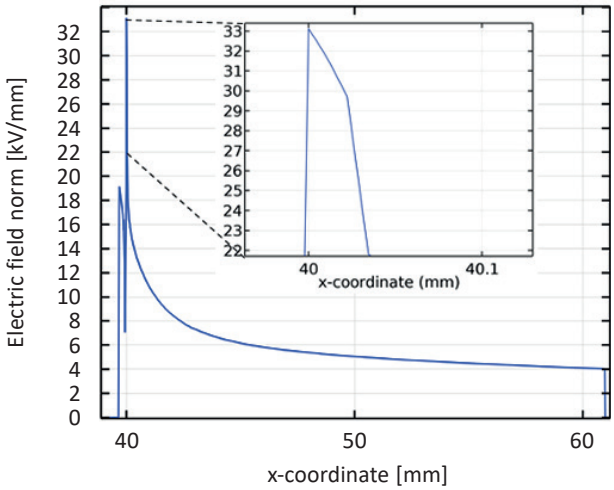

Fig. 16. Electric field plot of the 50 μm gas-filled spherical void outside the 3 mm spherical protrusion located at the conductor screen

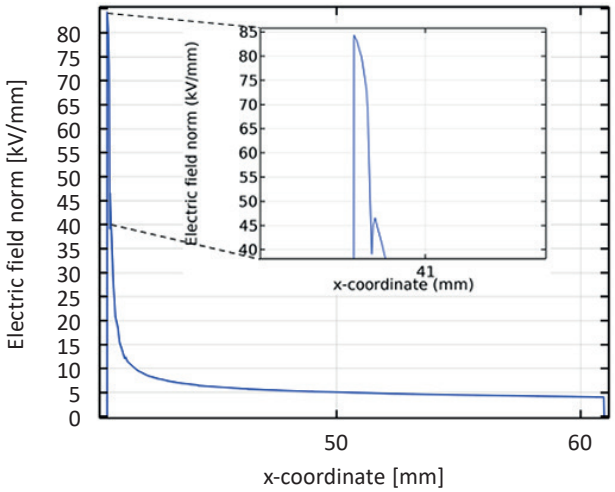

Fig. 18. Electric field distribution of the 1.5 mm long vented water tree grown from the 3 mm spherical protrusion located at the conductor screen

more than when the 3 mm spherical protrusion was examined in the absence of the void (2.16). This means that because of the low relative permittivity of voids compared to XLPE the manifestation of partial discharges would be at a higher degree leading to the deterioration of the insulating medium.

6.3. Analysis of protrusions with vented water trees (Case 3). Figures 17 and 18 show that the 1.5 mm long water tree also causes the intensification of the electric field compared to when the 3 mm spherical protrusion was present, but the vented water tree was absent (see Fig. 8). This is due to a variable permittivity within the vented water causing this increase and because of that, the generation of space charges will also increase. However, at the base (at 38.8 mm) of the water tree (tip of the protrusion) there was a substantial fall in the electric field because according to the assumptions made in case 3; the relative permittivity at the base is 5 which is larger than the permittivity of XLPE and the protrusion itself. However, after the base (after 38.8 mm), a decrease in the permittivity was assumed which is why the electric field amplified dramatically again after 38.8 mm. Then a drop was observed again because of less sharpness in the geometry of the water tree but another spike appears at 40.8 mm. This is because the tip of the water tree shows a substantial increase in the space charge density would accumulate at the sharper (tip) region of the water tree leading to this escalation in the electric field. Furthermore, the stress enhancement factor obtained was 12.6, which shows that the electric field increased more with the presence of vented water trees as opposed to its absence (2.16 previously in Fig. 10). As mentioned before the edge of the protrusion in contact with the conductor screen and the different permittivity between the conductor screen and the XLPE insulation causes the electric stress in the insulation to rise. This leads to the inception of treeing. Therefore, this is why this paper considers vented water trees growing from protrusions as the results obtained proves with full certainty that water trees can grow in the presence of protrusions and can put the insulation material in danger.

It is worth mentioning that from the space charge distribution, one can obtain an approximate value of the conductivity and permittivity of the vented water tree [26]. According to [26], the conductivity of water trees is approximately more than 10^6 higher than the XLPE without water trees according to the calculations done. The permittivity rise is merely observed in few instances.

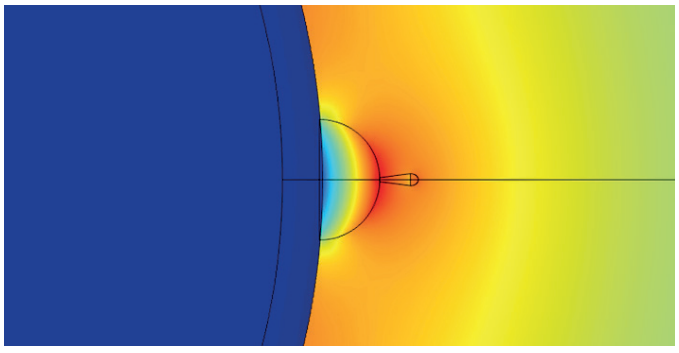

Fig. 17. Electric field distribution of the 1.5 mm long vented water tree grown from the 3 mm spherical protrusion located at the conductor screen

7. Conclusion

This paper focused on a COMSOL Multiphysics modelling of protrusions as defects or imperfections in an XLPE high voltage cable to examine the impact they have on the electric field distribution and the stress enhancement factor. Then a spherical gas-filled void was placed inside and outside a 3 mm protrusion, and a vented water tree grown from this particular protrusion was also considered. A DC high voltage was applied. When the sizes of the spherical and ellipsoidal protrusions increased the partial discharge activity and the stress enhancement factor also increased. When the void was placed inside and outside the 3 mm spherical protrusion, the electric field and the stress

enhancement factor were higher than when it was absent. However, the void placed outside the protrusion leads to a higher electric field versus to the one placed inside. When the water tree grown from the protrusion was considered a rise in the partial discharge activity was observed as suggested by the internal stress and the stress enhancement factor plotted. Ultimately, this paper proved the importance of considering multiple defects like the vented water tree growing from the protrusion because in practice the initiation of partial discharges due to protrusions, in fact, leads to treeing.

The novelty here lies in the fact that the edge of the protrusion at the conductor screen and the different permittivity between the conductor screen and the XLPE insulation causes the partial discharge activity in the insulation to rise, resulting in treeing. Therefore, vented water trees growing from protrusions were considered here as the process described proves that water trees can grow in the presence of protrusions. Otherwise, if the appropriate countermeasures are not considered, the discharge channel will grow to the opposite electrode until the two electrodes are electrically connected and that ultimately will lead to the breakdown of the insulation material.

Another contribution of the paper was to correct the fact that authors in literature usually consider air-filled voids rather than gas-filled voids. Due to the development of cables and the triple extrusion that takes place, it is not possible to introduce air, but gas inclusions can take place from by-products of the cross-linking process.

Acknowledgements. This publication was made possible by the NPRP grant [10-0101-170085] from the Qatar National Research Fund (a member of Qatar Foundation). The statements made herein are solely the responsibility of the authors.

References

[1] S.M.S. Tohid Shahsavarian, "Modelling of aged cavities for partial discharge in power cable insulation", *IET Sci. Meas. Technol.* 9(6), 661–670, 2015.

[2] M.A. Saleh and S.S. Refaat, "The Impact of Water Trees and Cavities on the Electric Field Distribution in XLPE Power Cables", in *2019 2nd International Conference on Smart Grid and Renewable Energy (SGRE)*, Doha, Qatar, 2019, pp. 1–8.

[3] N. Hampton, "Chapter 3: HV and EHV Cable System Aging and Testing Issues", *National Electric Energy Testing, Research and Applications Center,* no. Feb. pp. 1–19, 2016.

[4] T.L. Hanley, R.P. Burford, R.J. Fleming, and K.W. Barber, "A general review of polymeric insulation for use in HVDC cables", in *IEEE Electr. Insul. Mag.* 19(1), 13–24, (2003).

[5] W. Guoming and G.-S. Kil, "Measurement and Analysis of Partial Discharge Using an Ultra-High Frequency Sensor for Gas Insulated Structures", *Metrol. Meas. Syst.* 24 (3), 515–524 (2017).

[6] K.Ch. Kao, "Electrical Aging, Discharge, and Breakdown Phenomena", in *Dielectric Phenomena in Solids*, Ed(s): Kwan Chi Kao, pp. 515–572, Academic Press, 2004.

[7] J. Vedral and M. Kříž. "Signal Processing in Partial Discharge Measurement." *Metrol. Meas. Syst.* XVII (1), 55−64 (2010).

[8] S. Gutierrez, I. Sancho, L. Fontan, and J. D. No, "Effect of protrusions in HVDC cables", in *IEEE Trans. Dielectr. Electr. Insul.* 19(5), 1774–1781 (2012).

[9] M.S. Amir and S.M.H. Hosseini, "Comparison of aged XLPE power cables restoration by injecting two various anti-failure nanofluids", *Eng. Failure Anal.* 90, 262–276 (2018).

[10] L. Andrei, I. Vlad, and F. Ciuprina, "Electric field distribution in power cable insulation affected by various defects", in *2014 International Symposium on Fundamentals of Electrical Engineering (ISFEE)*, Bucharest, 2014, pp. 1–5.

[11] P.H.F. Morshuis, "Degradation of solid dielectrics due to internal partial discharge: Some thoughts on progress made and where to go now", *IEEE Trans. Dielectr. Electr. Insul.* 12(5), 905–913 (2005).

[12] P. Notingher, S. Holé, L. Berquez, and G.Teyssedre, "An Insight into Space Charge Measurements", *Int. J. Plasma Environ. Sci. Technol.* 11, 26–37 (2017).

[13] D.A. do Nascimento, S.S. Refaat, A. Darwish, Q. Khan, H. Abu-Rub, and Y. Iano, "Investigation of Void Size and Location on Partial Discharge Activity in High Voltage XLPE Cable Insulation", in *2019 Workshop on Communication Networks and Power Systems (WCNPS)*, Brasilia, Brazil, 2019, pp. 1–6.

[14] Z. Lei, J. Song, M. Tian, X. Cui, C. Li, and M. Wen, "Partial discharges of cavities in ethylene propylene rubber insulation", *IEEE Trans. Dielectr. Electr. Insul.* 21(4), 1647–1659 (2014).

[15] M. Mahdipour, A. Akbari, and P. Werle, "Charge concept in partial discharge in power cables", *IEEE Trans. Dielectr. Electr. Insul.* 24(2), 817–825 (2017).

[16] D. He, W. Wang, J. Lu, G. Teyssedre, and C. Laurent, "Space charge characteristics of power cables under AC stress and temperature gradients", *IEEE Trans. Dielectr. Electr. Insul.* 23(4), 2404–2412 (2016).

[17] M. Fu, L.A. Dissado, G. Chen, and J.C. Fothergill, "Space charge formation and its modified electric field under applied voltage reversal and temperature gradient in XLPE cable", *IEEE Trans. Dielectr. Electr. Insul.* 15(3), 851–860 (2008).

[18] R. Ross, "Inception and propagation mechanisms of water treeing", *IEEE Trans. Dielectr. Electr. Insul.* 5(5), 660–680, (1998).

[19] T. Boonraksa and B. Marungsri, "Role of Ionic Solutions Affect Water Treeing Propagation in XLPE Insulation for High Voltage Cable", *Int. J. Electr. Comput. Eng.* 8(5) 795–798 (2014).

[20] G. Callender, *Modelling Partial Discharge in Gaseous Voids by George Callender*, University of Southampton, 2018.

[21] G. Callender, P. Rapisarda, and P.L. Lewin, "Improving models of partial discharge activity using simulation", in *2017 IEEE Electr. Insul. Conf. EIC 2017*, 2017, pp. 392–395.

[22] X. Zhou, J. Cao, S. Wang, Y. Jiang, T. Li, and Y. Zou, "Simulation of electric field around typical defects in 110kV XLPE power cable joints", in *2017 International Conference on Circuits, Devices and Systems (ICCDS)*, Chengdu, 2017, pp. 21–24.

[23] L. Andrei, I. Vlad, and F. Ciuprina, "Electric field distribution in power cable insulation affected by water trees", in *2015 9th International Symposium on Advanced Topics in Electrical Engineering (ATEE)*, Bucharest, 2015, pp. 426–429.

[24] S. Gutiérrez, I. Sancho, L. Fontán, and M. Martínez-Iturralde, "Influence of irregularities within electric fields in high voltage cables", in *2011 Annual Report Conference on Electrical Insulation and Dielectric Phenomena*, Cancun, 2011, pp. 752–755.

[25] S. Nakamura, T. Ozaki, N. Ito, I. Sengoku, J. Kawai "Dynamic behavior of interconnected channels in water-treed polyethylene subjected to high voltage", *IEEE Trans. Dielectr. Electr. Insul.* 9, 390–395 (2002).

[26] T. Toyoda, S. Mukai, Y. Ohki, Y. Li, and T. Maeno, "Conductivity and permittivity of water tree in polyethylene", in *1999 Annual Report Conference on Electrical Insulation and Dielectric Phenomena (Cat. No.99CH36319)*, Austin, TX, USA, 1999, 577–580, vol. 2.